

Diagnosis of pseudoprogression in patients with glioblastoma using *O*-(2-[¹⁸F]fluoroethyl)-L-tyrosine PET

Norbert Galldiks · Veronika Dunkl · Gabriele Stoffels · Markus Hutterer · Marion Rapp · Michael Sabel · Guido Reifenberger · Sied Kebir · Franziska Dorn · Tobias Blau · Ulrich Herrlinger · Peter Hau · Maximilian I. Ruge · Martin Kocher · Roland Goldbrunner · Gereon R. Fink · Alexander Drzezga · Matthias Schmidt · Karl-Josef Langen

Received: 29 August 2014 / Accepted: 3 November 2014 / Published online: 20 November 2014
© Springer-Verlag Berlin Heidelberg 2014

Abstract

Purpose The follow-up of glioblastoma patients after radiochemotherapy with conventional MRI can be difficult since reactive alterations to the blood–brain barrier with contrast enhancement may mimic tumour progression (i.e. pseudoprogression, PsP). The aim of this study was to assess the clinical value of *O*-(2-¹⁸F-fluoroethyl)-L-tyrosine (¹⁸F-FET) PET in the differentiation of PsP and early tumour progression (EP) after radiochemotherapy of glioblastoma.

Methods A group of 22 glioblastoma patients with new contrast-enhancing lesions or lesions showing increased enhancement (>25 %) on standard MRI within the first 12 weeks after completion of radiochemotherapy with concomitant temozolomide (median 7 weeks) were additionally examined using amino acid PET with ¹⁸F-FET. Maximum and mean tumour-to-brain ratios (TBR_{max}, TBR_{mean}) were determined. ¹⁸F-FET uptake kinetic parameters (i.e. patterns of time–activity curves, TAC) were also evaluated. Classification as PsP or EP was based on the clinical course (no treatment change at

Norbert Galldiks and Veronika Dunkl contributed equally to this work.

N. Galldiks · V. Dunkl · G. R. Fink
Department of Neurology, University of Cologne, Cologne, Germany

N. Galldiks (✉) · V. Dunkl · G. Stoffels · G. R. Fink · K.-J. Langen
Institute of Neuroscience and Medicine, Forschungszentrum Jülich, 52425 Jülich, Germany
e-mail: Norbert.Galldiks@uk-koeln.de

N. Galldiks · U. Herrlinger · M. I. Ruge · M. Kocher · R. Goldbrunner
Center of Integrated Oncology (CIO), University of Cologne, Cologne, Germany

M. Hutterer · P. Hau
Department of Neurology and Wilhelm Sander-NeuroOncology Unit, University of Regensburg, Regensburg, Germany

M. Rapp · M. Sabel
Department of Neurosurgery, Heinrich Heine University Düsseldorf, Düsseldorf, Germany

G. Reifenberger
Department of Neuropathology, Heinrich Heine University Düsseldorf, Düsseldorf, Germany

S. Kebir · U. Herrlinger
Department of Neurology, University of Bonn, Bonn, Germany

F. Dorn
Department of Neuroradiology, University of Cologne, Cologne, Germany

T. Blau
Department of Neuropathology, University of Cologne, Cologne, Germany

M. I. Ruge
Department of Stereotaxy and Functional Neurosurgery, University of Cologne, Cologne, Germany

M. Kocher
Department of Radiation Oncology, University of Cologne, Cologne, Germany

R. Goldbrunner
Department of Neurosurgery, University of Cologne, Cologne, Germany

A. Drzezga · M. Schmidt
Department of Nuclear Medicine, University of Cologne, Cologne, Germany

K.-J. Langen
Department of Nuclear Medicine, University of Aachen, Aachen, Germany

least for 6 months), follow-up MR imaging and/or histopathological findings. Imaging results were also related to overall survival (OS).

Results PsP was confirmed in 11 of the 22 patients. In patients with PsP, ^{18}F -FET uptake was significantly lower than in patients with EP (TBR_{max} 1.9 ± 0.4 vs. 2.8 ± 0.5 , TBR_{mean} 1.8 ± 0.2 vs. 2.3 ± 0.3 ; both $P < 0.001$) and presence of MGMT promoter methylation was significantly more frequent ($P = 0.05$). Furthermore, a TAC type II or III was more frequently present in patients with EP ($P = 0.04$). Receiver operating characteristic analysis showed that the optimal ^{18}F -FET TBR_{max} cut-off value for identifying PsP was 2.3 (sensitivity 100 %, specificity 91 %, accuracy 96 %, AUC 0.94 ± 0.06 ; $P < 0.001$). Univariate survival analysis showed that a $\text{TBR}_{\text{max}} < 2.3$ predicted a significantly longer OS (median OS 23 vs. 12 months; $P = 0.046$).

Conclusion ^{18}F -FET PET may facilitate the diagnosis of PsP following radiochemotherapy of glioblastoma.

Keywords Pseudoprogression · Tumour progression · Glioblastoma · FET PET

Introduction

Within the first 12 weeks after completion of radiotherapy (usually radiochemotherapy with concomitant temozolomide), patients with a high-grade brain tumour can present with an enlarged area of contrast enhancement on MRI, followed by subsequent improvement or stabilization without any change in treatment [1]. This phenomenon, which mimics tumour progression, has been termed “pseudoprogression” (PsP) and is a consequence of a subacute treatment-related local tissue reaction which comprises inflammation, oedema and increased permeability of the blood–brain barrier [2]. Importantly, PsP occurs with or without clinical deterioration, even though in most patients PsP remains asymptomatic [3]. Interestingly, PsP seems to be associated with a better outcome and is more common in patients whose tumour shows a methylated O⁶-methylguanine DNA methyltransferase (MGMT) gene promoter [4] and thus are more responsive to temozolomide treatment [5]. The period of stabilization after PsP typically ranges between 3 and 6 months [2], although single cases with late onset of PsP followed by a prolonged radiological improvement have been observed, especially after chemotherapy using temozolomide in combination with lomustine [6]. Clinically, PsP is of considerable importance in neurooncology since it occurs in 15–30 % of patients with malignant glioma [3, 7], and in patients with concomitant clinical deterioration a successful treatment might be erroneously terminated with a potentially negative influence on survival.

After treatment, conventional MRI cannot reliably differentiate tumour recurrence from PsP [3, 7]. Radiation necrosis, tumour recurrence and PsP are able to cause a destabilization of the blood–brain barrier, resulting in nonspecific contrast enhancement on MRI. Furthermore, blood–brain barrier breakdown may result from postoperative inflammation, seizures, tumour recurrence or treatment effects.

In view of the described limitations of conventional MRI, metabolic imaging may provide valuable information [8, 9]. In particular, PET with amino acid tracers seems to be particularly useful in detecting PsP, as amino acid uptake is increased in tumour tissue but low or absent in areas of radiation-induced change [10, 11]. The most widely used tracer for amino acid PET is ^{11}C -methyl-L-methionine (^{11}C -MET), but its use is limited to PET centres with a cyclotron because of its short physical half-life (20 min) [12]. *O*-(2- ^{18}F -Fluoroethyl)-L-tyrosine (^{18}F -FET) is a well-established ^{18}F -labelled amino acid for PET (half-life 110 min) that shows logistic advantages over ^{11}C -MET in clinical practice [13]. Furthermore, differential ^{18}F -FET uptake kinetics have been observed in patients with high-grade and low-grade glioma and this seems to be a special property of this particular tracer, as similar features have not been observed with ^{11}C -MET [14].

Taking together the above considerations, we assessed the diagnostic value of ^{18}F -FET PET uptake ratios as well as ^{18}F -FET uptake kinetics for detection of PsP in patients with glioblastoma, the most common type of malignant glioma.

Materials and methods

Patients and treatment

Included in this retrospective study were 22 consecutive patients with supratentorial glioblastoma treated from 2009 to 2012. The local ethics committee approved the evaluation of retrospectively collected patient data. All patients exhibited a new lesion or enlargement of contrast-enhancing lesions on standard MRI (gadolinium-based contrast agent) within the first 12 weeks after completion of radiotherapy with concomitant temozolomide. In order to differentiate between PsP and early tumour progression (EP), standard MRI was followed by ^{18}F -FET PET imaging after a median of 7 days. The patients comprised 14 men and 8 women with a mean age of 56 years (range 34–76 years). Open resection was performed in 21 patients, with 9 surgical interventions being rated as partial resection and 12 as complete resection on early postoperative MRI within 48 h. Due to proximity of the tumour to critical or eloquent brain structures, one patient received diagnostic stereotactic biopsy but no open resection. Surgery or biopsy was followed by external fractionated radiotherapy (60 Gy) with concomitant temozolomide (75 mg/m^2 body surface area per

day, 7 days per week from the first to the last day of radiotherapy) and after a 4-week break adjuvant temozolomide chemotherapy (150–200 mg/m² body surface area over 5 days, repeated every 23 days, for six cycles) in accordance with the design of EORTC trial 22981/26981 [15]. During adjuvant temozolomide therapy, patients underwent a clinical evaluation every 8–12 weeks. Following completion of adjuvant temozolomide therapy, a clinical evaluation was performed every 2–3 months in each patient.

Diagnosis of pseudoprogression and early tumour progression

The diagnosis of PsP or EP was based on the criteria defined by Young et al. [7]. Lesions on the initial MRI scan that worsened within the first 12 weeks after completion of radiochemotherapy were categorized as either EP or PsP based on pathological analysis after repeated biopsy or resection when available (in 11 patients). PsP was characterized by prominent necrosis with no or minimal identifiable tumour remnants. The presence of recurrent tumour confirmed EP.

If no repeat pathology was available (in 11 patients), the clinical diagnosis of EP or PsP was reached via consensus of two experienced neurooncologists based upon a complete chart review and review of follow-up MR imaging. The diagnosis of PsP was assumed if no change in treatment was required for at least 6 months after the end of radiochemotherapy. This definition allows a continued mild increase in the worsening of enhancing lesions, as compared to the usual decrease or stabilization, as long as no treatment change occurred during this period. The diagnosis of EP was made if imaging or clinical worsening prompted a change in treatment. The classification was made without knowledge of the patient's MGMT promoter methylation status.

Histological tumour classification and analysis for MGMT promoter methylation

All tumours were histologically classified as glioblastoma of World Health Organization (WHO) grade IV according to the WHO classification of tumours of the central nervous system [16]. Tumour DNA extraction from formalin-fixed and paraffin-embedded tissue samples was carried out with the Qiagen blood and tissue DNA extraction kit (Qiagen, Hilden, Germany). Only tissue samples containing vital glioblastoma tissue with a histologically estimated tumour cell content of 80 % or more were used for DNA extraction. MGMT promoter methylation was assessed using a methylation-specific PCR as described elsewhere [17].

PET imaging with ¹⁸F-FET

All patients had given written informed consent to participation in the ¹⁸F-FET studies. The amino acid ¹⁸F-FET was

produced as described previously [18, 19]. According to the German guidelines for brain tumour imaging using labelled amino acid analogues, all patients fasted for at least 12 h before PET scanning [20]. Dynamic PET studies were acquired up to 50 min after intravenous injection of approximately 200 MBq ¹⁸F-FET on an ECAT EXACT HR+ scanner (Siemens Medical Systems) in three-dimensional mode (32 rings, axial field of view 15.5 cm). The emission recording consisted of 16 time frames (1–5, 1 min; 6–10, 3 min; and 11–16, 5 min) covering the period up to 50 min after injection. For attenuation correction, transmission was measured with three ⁶⁸Ge/⁶⁸Ga rotating line sources. After correction for random and scattered coincidences and dead time, 63 image planes were iteratively reconstructed (OSEM, six iterations, 16 subsets) using the ECAT 7.2 software. The resolution of the reconstructed images was approximately 5.5 mm.

PET data analysis

Tissue uptake was expressed as standardized uptake values (SUV) by dividing the radioactivity (kilobecquerels per millilitre) in the tissue by the radioactivity injected per gram of body weight. PET and MR images were coregistered using dedicated software (MPI tool version 6.48; ATV, Kerpen, Germany). The fusion results were inspected and if necessary adapted based on anatomical landmarks. The regions-of-interest (ROI) analysis was based on the summed PET data from 20 to 40 min after injection. The transaxial slices showing the highest tracer accumulation in the tumours were chosen for ROI analysis. The uptake in the unaffected brain tissue was determined by a larger ROI placed on the contralateral hemisphere in an area of normal-appearing brain tissue including white and grey matter [20]. Mean amino acid uptake in the tumour was determined using a two-dimensional autocontouring process with a tumour-to-brain ratio (TBR) of 1.6 as described previously [21]. For determination of maximal amino acid uptake a circular ROI with a diameter of 1.6 cm was centred on the maximal tumour uptake. If the autocontouring process yielded a ROI with a diameter <1.6 cm, a circular ROI with a diameter of 1.6 cm was applied. Mean and maximum TBRs (TBR_{mean}, TBR_{max}) were calculated by dividing the mean SUV of these tumour ROIs by the mean SUV of normal brain in the PET scan.

For ¹⁸F-FET PET, time-activity curves (TAC) of mean SUV in the tumour and in the brain were generated by application of a spherical volume of interest with a volume of 2 ml centred on the maximal tumour uptake and a reference ROI in the unaffected brain tissue (as described above) to the entire dynamic dataset. Time-to-peak (TTP; time in minutes from the beginning of the dynamic acquisition to the maximum SUV of the lesion) was determined. Furthermore, as previously described [22, 23], the TACs of each lesion were assigned to one of the following curve patterns: constantly increasing

^{18}F -FET uptake without identifiable peak uptake (pattern I); ^{18}F -FET uptake peaking at a mid-point (>20 – 40 min) followed by a plateau or a small descent (pattern II); and ^{18}F -FET uptake peaking early (≤ 20 min) followed by a constant descent (pattern III). The TACs were assigned to the various curve patterns by three experienced raters (N.G., K.J.L., G.S.).

MR imaging

At initial diagnosis and during the course of disease, all patients had a routine MRI scan using a 1.5-T MRI scanner with a standard head coil before and after administration of a gadolinium-based contrast agent (T1, T2 and FLAIR sequence). In order to evaluate the extent of tumour resection, an early postoperative MRI scan was performed within the first 48 h. The presence of contrast enhancement was considered as a partial resection, and absence as complete resection. The first follow-up MRI scan after radiochemotherapy was performed not before 3–4 weeks and not later than 12 weeks after completion of radiochemotherapy. During and after completion of adjuvant temozolomide therapy, patients underwent a follow-up contrast-enhanced MRI scan every 8–12 weeks.

Definition of survival times

Overall survival time (OS) was defined as the interval from date of initial surgery to date of death or, if the patients were still alive, as the interval from date of initial surgery to date of last contact.

Statistical analysis

Descriptive statistics are provided as means and standard deviations or as medians and ranges. To compare clinical conditions and amino acid PET parameters in patients with PsP and EP, Student's *t* test for independent samples was used. The Wilcoxon test was used when variables were not normally distributed. Survival analyses were performed using the log-rank test (univariate analysis) for OS (data presented as medians).

The diagnostic performance of ^{18}F -FET uptake as determined by TBR_{max} and TBR_{mean} to identify PsP was assessed by receiver operating characteristic (ROC) curve analysis using the histological confirmation or clinical course as reference. Decision cut-off was considered optimal when the product of paired values for sensitivity and specificity reached a maximum. In addition, the areas under the ROC curves (AUC) and their standard error and level of significance were determined as a measure of diagnostic quality. The diagnostic performance of ^{18}F -FET TAC patterns in combination with the corresponding TBRs was evaluated using the Fisher exact test for 2×2 contingency tables. After assignment of the TACs of ^{18}F -FET uptake to the three curve patterns Cohen's κ -test

was used to measure the degree of agreement among the raters (N.G., K.J.L., G.S.); κ values between 0 and 0.20 were considered to indicate a positive but slight correlation, between 0.21 and 0.40 a fair correlation, between 0.41 and 0.60 a good correlation, between 0.61 and 0.80 a very good correlation, and greater than 0.80 an excellent correlation.

P values of 0.05 or less were considered significant. Statistical analyses were performed using SigmaPlot software (SigmaPlot Version 11.0, Systat Software, San Jose, CA) and PASW statistics software (release 22.0.0; SPSS, Chicago, IL).

Results

Pseudoprogression and early progression

The first follow-up routine MRI scan after the end of radiochemotherapy was performed after a median of 7 weeks (range 3–8 weeks, mean 6 ± 2 weeks). At that time, MRI scans in all 22 patients suggested tumour recurrence/progression. PsP was confirmed in 11 of the 22 patients, i.e. a prevalence of 50 % in this particular patient group (Table 1). In 3 of the 11 patients with PsP (27 %), diagnosis was confirmed histologically. In 8 of the 11 patients (72 %) with EP, histological analysis was obtained and confirmed recurrent glioblastoma in each patient (Table 2). Significant group differences (PsP vs. EP) regarding age (58 ± 12 years vs. 53 ± 9 years; $P=0.29$) and extent of resection (complete vs. partial resection or biopsy; $P=0.16$) were not observed. Representative patient examples are presented in Figs. 1 and 2.

MGMT promoter methylation

Tumour specimens were available from 21 of the 22 patients for MGMT promoter methylation analysis. Eight of the 21 patients (38 %) had tumours with a methylated MGMT promoter and 13 had tumours without MGMT promoter methylation. In the group of patients with PsP, the presence of MGMT promoter methylation was significantly higher than in those with EP ($P=0.05$).

^{18}F -FET tracer uptake and ^{18}F -FET kinetics

TBR_{max} and TBR_{mean} of ^{18}F -FET uptake were significantly higher in patients with EP than in patients with PsP (TBR_{max} 2.8 ± 0.5 vs. 1.9 ± 0.4 , $P < 0.001$; TBR_{mean} 1.8 ± 0.2 vs. 2.3 ± 0.3 , $P < 0.001$; Tables 1 and 2). In patients with EP, the mean TTP was significantly shorter than in patients with PsP (mean TTP 26 ± 10 vs. 35 ± 9 min, $P=0.05$). Furthermore, a type II or III kinetic pattern was more frequently present in patients with EP ($P=0.04$). Detailed data on TTP and kinetic patterns in

Table 1 Glioblastoma patients with pseudoprogression

Patient	Gender	Age (years)	Extent of resection	MGMT promoter status	End of radiochemotherapy to first follow-up (weeks)	Progression-free survival (months)	Overall survival (months)	PET tracer	TBR _{max}	TBR _{mean}	Kinetic pattern	Time to peak (min)	Confirmation of pseudoprogression
1	F	71	Partial	Methylated	3	12	Lost to follow-up	¹⁸ F-FET	1.5	1.5	I	40	Histology
2	F	76	Complete	Methylated	8	21	21 ^a	¹⁸ F-FET	2.2	1.9	II	35	Histology
3	F	58	Partial	Unmethylated	8	24	28 ^a	¹⁸ F-FET	1.7	1.7	II	25	Clinical course
4	F	59	Complete	Unmethylated	8	14	16	¹⁸ F-FET	1.6	1.6	I	30	Clinical course
5	M	63	Complete	Methylated	8	9	20	¹⁸ F-FET	1.9	1.9	I	45	Clinical course
6	M	50	Complete	Unmethylated	4	16	23	¹⁸ F-FET	2.2	2.0	I	45	Clinical course
7	M	34	Partial	Methylated	8	17 ^a	17 ^a	¹⁸ F-FET	1.6	1.6	I	45	Clinical course
8	F	48	Complete	Not available	8	14 ^a	14 ^a	¹⁸ F-FET	1.7	1.7	II	25	Histology
9	F	64	Complete	Methylated	4	9 ^a	9 ^a	¹⁸ F-FET	1.5	1.5	I	45	Clinical course
10	M	70	Complete	Unmethylated	4	12	20	¹⁸ F-FET	2.7	2.1	II	25	Clinical course
11	M	48	Complete	Methylated	4	22	23 ^a	¹⁸ F-FET	2.2	1.9	II	25	Clinical course

^a Not reached, patient still free of progression/alive at the time of this report

patients with PsP and EP are presented in Tables 1 and 2. There was excellent interobserver agreement in the assignment of TACs to the three curve patterns with a mean κ value of 0.83±0.09 (range 0.78–0.93).

ROC analysis

The ROC analysis showed that the optimal ¹⁸F-FET TBR_{max} cut-off value for identifying PsP was 2.3 (sensitivity 100 %, specificity 91 %, accuracy 96 %, AUC 0.94±0.06; *P*<0.001). The corresponding TBR_{mean} cut-off value for identifying PsP was 2.0 (sensitivity 82 %, specificity 82 %, accuracy 82 %, AUC 0.91±0.06; *P*=0.001; Table 3). The combined analysis of ¹⁸F-FET PET parameters (presence of TBR_{max} >2.3 in combination with kinetic pattern II or III) best differentiated EP from PsP with a sensitivity of 80 %, a specificity of 91 % and an accuracy of 86 % (*P*=0.002). TBR_{mean} >2.0 in combination with kinetic pattern II or III yielded a sensitivity of 60 %, a specificity of 91 % and an accuracy of 76 % (*P*=0.024; Table 3).

Survival

Patients with PsP demonstrated a significantly longer OS than patients with EP (median OS 16 vs. 8 months; *P*=0.006). In univariate survival analysis, the presence of TBR_{max} <2.3 predicted a significantly longer OS (median OS 23 vs. 12 months; *P*=0.046; Fig. 3).

Discussion

The finding of new or enlarging contrast-enhancing lesions on standard MRI within the first 12 weeks after completion of radiochemotherapy has limited diagnostic value in differentiating PsP and EP in patients with glioblastoma. However, the reliable differentiation of EP from PsP is crucial since PsP spontaneously resolves without changing the standard treatment and a correct diagnosis may prevent unnecessary and potentially harmful change in treatment. On the other hand, the reliable detection of tumour progression at an early stage is essential for optimizing the treatment strategy in the individual patient. Young et al. screened a cohort of 93 glioblastoma patients for structural MRI findings that might be helpful for differentiating between PsP and EP [7]. However, they failed to identify such features in morphological MR scans that could be of value in clinical routine. While subependymal spread of the enhancing lesion seemed to be a useful MRI marker in identifying EP, the sensitivity of this finding was low (38 %). Therefore, a number of novel imaging methods are currently under clinical evaluation seeking to overcome the limitations of conventional MRI and to achieve reliable differentiation of PsP and EP with high diagnostic accuracy.

Table 2 Glioblastoma patients with early tumour progression (progression-free survival ≤ 6 months)

Patient	Gender	Age (years)	Extent of resection	MGMT promoter status	End of radiochemotherapy to first follow-up MRI (weeks)	Progression-free survival (months)	Overall survival (months)	PET tracer	TBR _{max}	TBR _{mean}	Kinetic pattern	Time to peak (min)	Confirmation of early tumour progression	Treatment of early progression
1	F	42	Partial	Unmethylated	6	4	21 ^a	¹⁸ F-FE- ^T	2.4	2.4	Not available		Histology	PC
2	M	57	Partial	Unmethylated	6	4	9	¹⁸ F-FE- ^T	2.4	2.0	III	20	Histology	Resection, TMZ
3	M	61	Complete	Unmethylated	4	5	Lost to follow-up	¹⁸ F-FE- ^T	3.6	2.2	I	40	Histology	Resection
4	M	52	Partial	Unmethylated	4	5	12	¹⁸ F-FE- ^T	2.6	2.6	II	30	Histology	Resection, TMZ
5	M	59	Partial	Unmethylated	8	6	12	¹⁸ F-FE- ^T	2.4	2.3	II	25	Histology	Resection, RCx, TMZ
6	F	43	Complete	Unmethylated	8	5	16 ^a	¹⁸ F-FE- ^T	2.4	1.9	II	30	Clinical course	BEV
7	M	52	Complete	Unmethylated	7	5	12 ^a	¹⁸ F-FE- ^T	2.6	1.9	II	30	Clinical course	BEV
8	M	72	Biopsy only	Unmethylated	7	4	7	¹⁸ F-FE- ^T	3.6	2.7	III	20	Clinical course	CCNU
9	M	51	Partial	Methylated	6	5	6 ^a	¹⁸ F-FE- ^T	3.6	2.7	III	8	Histology	Resection, TMZ
10	M	44	Complete	Unmethylated	3	3	8 ^a	¹⁸ F-FE- ^T	2.6	2.0	I	40	Histology	Resection, BEV
11	M	53	Partial	Methylated	8	5	12	¹⁸ F-FE- ^T	2.8	2.1	III	20	Histology	Resection, BEV

PC procarbazine and lomustine, TMZ temozolomide 150–200 mg/m body surface area over 5 days, repeated every 23 days, RCx radiochemotherapy with concomitant temozolomide, BEV bevacizumab, CCNU lomustine

^a Not reached, patient still alive at the time of this report

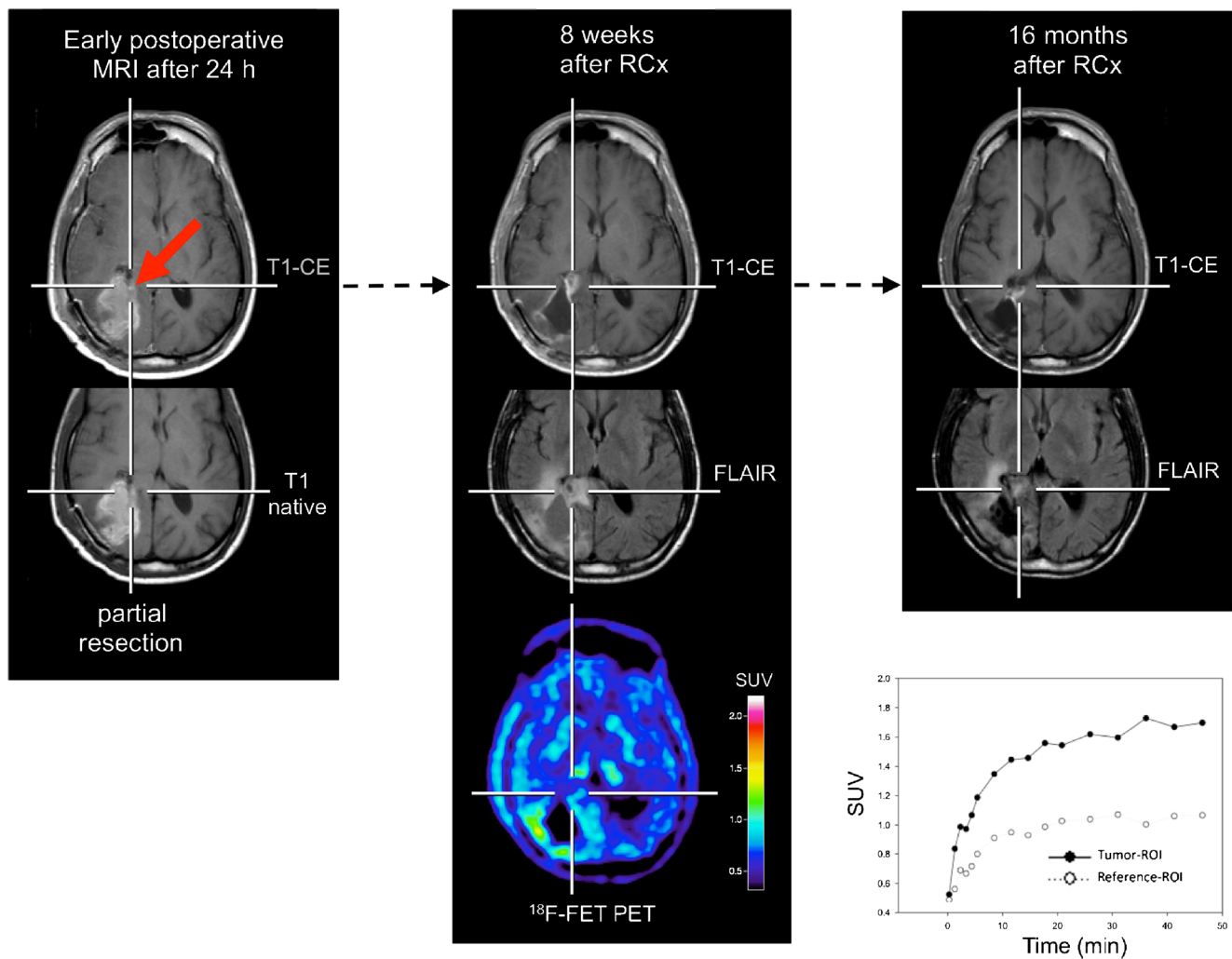


Fig. 1 PET and MR imaging in a 34-year-old glioblastoma patient (patient 7, pseudoprogression group, MGMT promoter methylated) 24 h after resection, and 8 weeks and 16 months after completion of radiochemotherapy (RCx). The early postoperative MR images (*left*) show a small point-shaped residual contrast-enhancing tumour in the right parietooccipital area (*red arrow*, diameter 5 mm). The follow-up MRI images 8 weeks after completion of radiochemotherapy suggest tumour progression (*middle column, top image*). In contrast, in the area

spatially corresponding to the enlarged contrast enhancement, the ^{18}F -FET PET image shows no metabolically active tumour. Dorsolateral to the resection hole, slightly increased metabolic activity (TBR_{max} 1.6) with ^{18}F -FET uptake kinetic pattern I is present. Follow-up MR images after 16 months show a slightly reduced contrast enhancement and FLAIR signal alteration (*right column*). After a follow-up of 17 months without any change in treatment, the patient was still alive, clinically stable and free of tumour progression

PET studies using ^{18}F -FET have been shown to provide valuable information for the diagnostic assessment of cerebral gliomas. ^{18}F -FET PET offers a more precise delineation of the “true” extent of glioblastoma, i.e. the metabolically active tumour, which is not limited to the area of blood–brain barrier disruption and is more specific than the information provided by conventional MRI alone [24]. Furthermore, ^{18}F -FET PET has been shown to be helpful for treatment monitoring [10, 25, 26], detection of malignant progression [23], prognostication [27], differential diagnosis [21, 28], and the differentiation of tumour recurrence and radiation-induced changes [10, 11, 29]. Therefore, there are reasonable grounds to believe that this method may have potential to differentiate PsP from EP in patients with glioblastoma.

The present study demonstrated that ^{18}F -FET uptake TBRs and also tracer kinetics provide valuable clinical information for the differentiation of PsP from EP in glioblastoma patients within the first 12 weeks after radiotherapy with concomitant temozolomide, which could not be derived from conventional MRI based on Response Assessment in Neuro-Oncology criteria [1] (Figs. 1 and 2). A TBR_{max} threshold of 2.3 allowed differentiation between PsP and EP with the highest diagnostic accuracy of 96 % (sensitivity 100 %, specificity 91 %). The combined analysis of static and kinetic ^{18}F -FET uptake provided no further improvement in diagnostic accuracy. A final decision concerning the additional value of static and kinetic ^{18}F -FET PET for the differentiation of PsP from EP early after completion of radiochemotherapy

should be made after confirmation in a larger series of patients.

It has to be considered that patients were admitted to our department for the differentiation of EP from PsP from different neighbouring university hospitals with the neurooncological focus depending on the availability of a timely appointment of ^{18}F -FET PET and clinical need. Probably, referring centres admitted mainly patients in whom the clinical findings and MRI scan were particularly ambiguous. This possible selection bias, however, does not present a drawback for the study because ^{18}F -FET PET will be considered as an additional tool especially when the diagnosis is unclear on the basis of conventional imaging.

Furthermore, the diagnostic impact of ^{18}F -FET PET needs to be compared with advanced MR imaging techniques such

as perfusion-weighted and diffusion-weighted imaging (PWI, DWI) to differentiate EP from PsP [30–32]. Using DWI, the apparent diffusion coefficient (ADC) values are higher in areas of posttreatment change than in recurrent/progressive tumour tissue because of the high cellularity of tumour tissue [33]. Using PWI, the regional cerebral blood volume (rCBV), which is assumed to reflect neovascularization and viable tumour, can be determined [34]. Kong et al. reported that the sensitivity and specificity of rCBV ratios at a certain threshold for differentiating PsP from tumour progression are 82 % and 78 %, respectively [31]. In relation to the diagnostic accuracy of ^{18}F -FET PET of 96 % observed in this study, PWI appears to be clearly inferior to amino acid PET. Using more sophisticated evaluation methods, i.e. histogram analysis, the diagnostic performance of rCBV imaging can be slightly

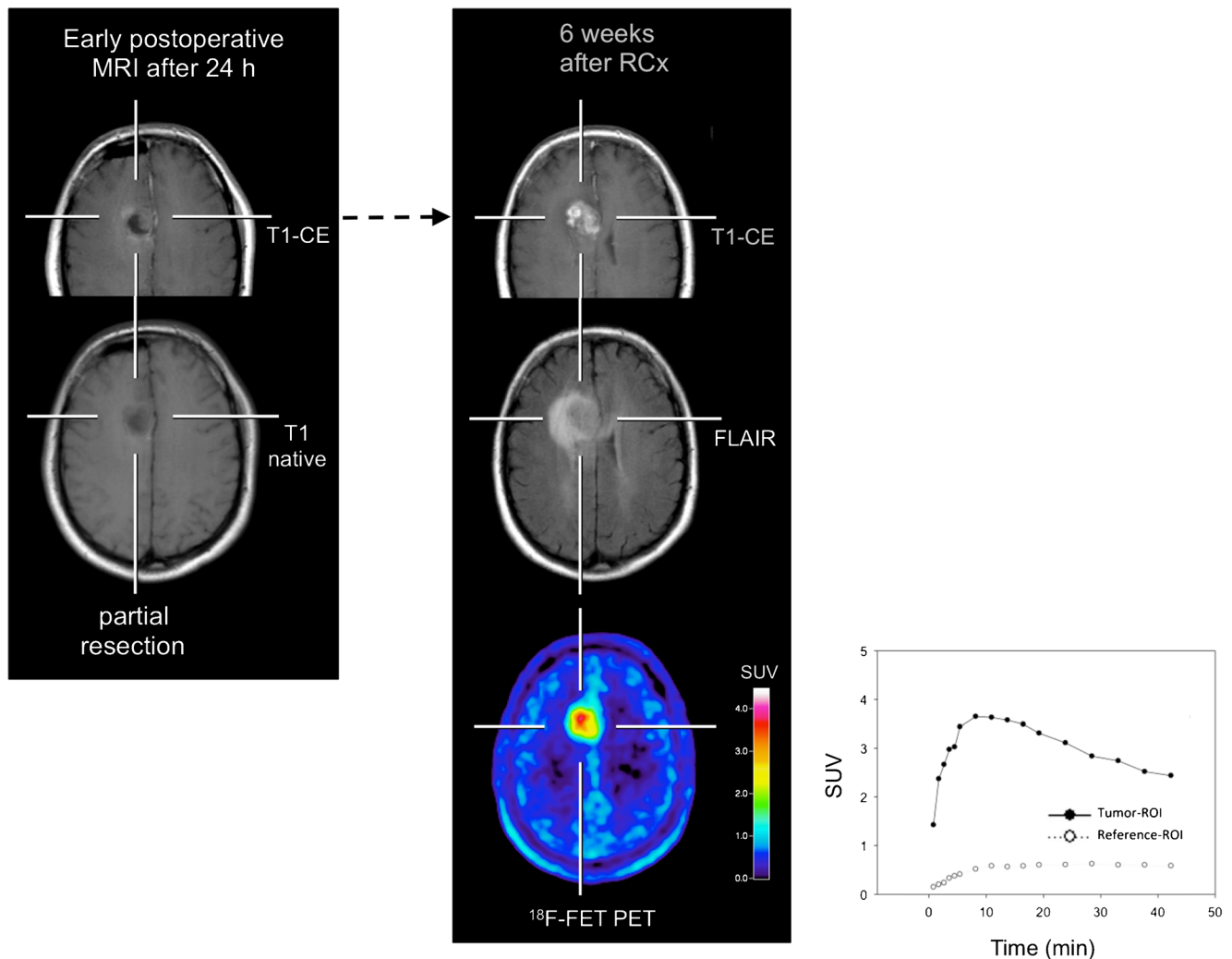


Fig. 2 PET and MR imaging in a 51-year-old glioblastoma patient 24 h after resection and 6 weeks after completion of radiochemotherapy (patient 9, early tumour progression group). The early postoperative MR images (*left column*) show a residual contrast-enhancing lesion, consistent with a partial tumour resection. The follow-up MRI images 6 weeks

after completion of radiochemotherapy suggest local tumour progression (*right column*). In the spatially corresponding area, the ^{18}F -FET PET image shows a metabolically active tumour (TBR_{max} 3.6) with ^{18}F -FET uptake kinetic pattern III. The patient underwent surgery and the diagnosis of tumour progression was confirmed histologically

Table 3 Diagnostic performance of imaging parameters at their best threshold (TBR_{max} 2.3, TBR_{mean} 2.0) for differentiating pseudoprogression from early progression

Diagnostic performance	TBR _{max}	TBR _{mean}	Combined analysis ^a		New occurrence/increase >25 % of contrast enhancement on MRI
			TBR _{max}	TBR _{mean}	
Sensitivity (%)	100 (95 % CI 89–100)	82 (95 % CI 70–94 %)	80	60	100
Specificity (%)	91 (95 % CI 80–100)	82 (95 % CI 70–94 %)	91	91	–
Accuracy (%)	96	82	86	76	54
AUC±standard error	0.94±0.06 (0.83–1)	0.90±0.07 (0.80–1)	Not available	Not available	Not available
P value	< 0.001	0.001	0.002	0.024	Not available

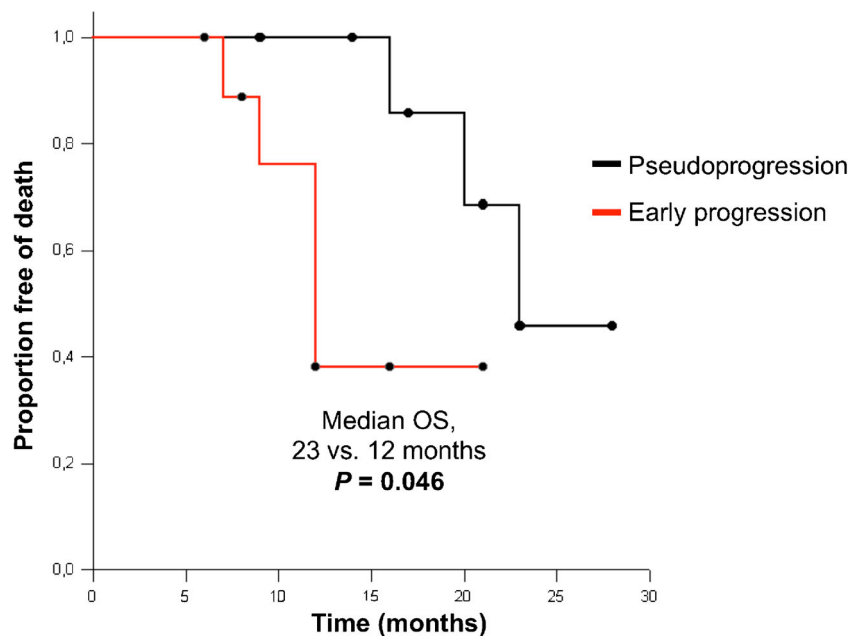
^aTBR_{max} 2.3 or TBR_{mean} 2.0 in combination with kinetic pattern II or III

increased (range of sensitivity 86–90 %, range of specificity 89–91 %) [35, 36]. A multiparametric approach combining DWI, PWI and histogram analysis has yielded a further improvement in specificity (100 %), albeit at a lower sensitivity (82 %) [30]. A major limitation of rCBV for evaluation of PsP is that treatment-related inflammation also causes increased rCBV. In patients with radiation-induced changes, e.g. radiation necrosis, local inflammatory responses with infiltration of lymphocytes and macrophages may result in increased rCBV [37]. On DWI, radiation-induced necrosis may also show diffusion restriction, probably due to intracellular oedema and viscous pus-like material with leucocyte infiltrates in the transition zone [33]. Therefore, increased rCBV is not necessarily associated with tumour angiogenesis, and decreased ADC values do not always reflect high cellularity.

Conclusion

In summary, our data suggest that ¹⁸F-FET PET in glioblastoma patients is a promising method for overcoming the limitations of conventional MRI in differentiating PsP from EP. In future studies, the additive diagnostic value of both amino acid PET and advanced MRI techniques should be investigated in order to achieve the best diagnostic accuracy in this crucial clinical problem. The detection of tumour progression at an early stage is essential to optimize the treatment strategy in each individual patient. In order to provide the optimal diagnostic approach to the individual patients, multimodal imaging trials should be implemented on the basis of reader-independent image analysis and carried out as multicentre trials. From these trials, surrogate imaging parameters should be derived that can then be used in routine clinical practice.

Fig. 3 Univariate survival analysis, TBR_{max} <2.3 (patients with pseudoprogression) predicts a significantly longer OS (median OS 23 vs. 12 months; P=0.046)



Conflicts of interest None.

References

- Wen PY, Macdonald DR, Reardon DA, Cloughesy TF, Sorensen AG, Galanis E, et al. Updated response assessment criteria for high-grade gliomas: response assessment in neuro-oncology working group. *J Clin Oncol*. 2010;28:1963–72.
- Brandsma D, van den Bent MJ. Pseudoprogression and pseudoresponse in the treatment of gliomas. *Curr Opin Neurol*. 2009;22:633–8.
- Brandsma D, Stalpers L, Taal W, Sminia P, van den Bent MJ. Clinical features, mechanisms, and management of pseudoprogression in malignant gliomas. *Lancet Oncol*. 2008;9:453–61.
- Brandes AA, Franceschi E, Tosoni A, Blatt V, Pession A, Tallini G, et al. MGMT promoter methylation status can predict the incidence and outcome of pseudoprogression after concomitant radiochemotherapy in newly diagnosed glioblastoma patients. *J Clin Oncol*. 2008;26:2192–7.
- Hegi ME, Diserens AC, Gorlia T, Hamou MF, de Tribolet N, Weller M, et al. MGMT gene silencing and benefit from temozolomide in glioblastoma. *N Engl J Med*. 2005;352:997–1003.
- Stuplich M, Hadizadeh DR, Kuchelmeister K, Scorzin J, Filss C, Langen KJ, et al. Late and prolonged pseudoprogression in glioblastoma after treatment with lomustine and temozolomide. *J Clin Oncol*. 2012;30:e180–3.
- Young RJ, Gupta A, Shah AD, Graber JJ, Zhang Z, Shi W, et al. Potential utility of conventional MRI signs in diagnosing pseudoprogression in glioblastoma. *Neurology*. 2011;76:1918–24.
- Yang I, Aghi MK. New advances that enable identification of glioblastoma recurrence. *Nat Rev Clin Oncol*. 2009;6:648–57.
- Yang I, Huh NG, Smith ZA, Han SJ, Parsa AT. Distinguishing glioma recurrence from treatment effect after radiochemotherapy and immunotherapy. *Neurosurg Clin N Am*. 2010;21:181–6.
- Galldiks N, Langen K, Holy R, Pinkawa M, Stoffels G, Nolte K, et al. Assessment of treatment response in patients with glioblastoma using [18F]fluoroethyl-L-tyrosine PET in comparison to MRI. *J Nucl Med*. 2012;53:1048–57.
- Rachinger W, Goetz C, Pöpperl G, Gildehaus FJ, Kreth FW, Holtmannspotter M, et al. Positron emission tomography with O-(2-[18F]fluoroethyl)-L-tyrosine versus magnetic resonance imaging in the diagnosis of recurrent gliomas. *Neurosurgery*. 2005;57:505–11.
- Herholz K, Langen KJ, Schiepers C, Mountz JM. Brain tumors. *Semin Nucl Med*. 2012;42:356–70.
- Langen KJ, Hamacher K, Weckesser M, Floeth F, Stoffels G, Bauer D, et al. O-(2-[18F]fluoroethyl)-L-tyrosine: uptake mechanisms and clinical applications. *Nucl Med Biol*. 2006;33:287–94.
- Moulin-Romsée G, D'Hondt E, de Groot T, Goffin J, Sciot R, Mortelmans L, et al. Non-invasive grading of brain tumours using dynamic amino acid PET imaging: does it work for 11C-methionine? *Eur J Nucl Med Mol Imaging*. 2007;34:2082–7.
- Stupp R, Mason WP, van den Bent MJ, Weller M, Fisher B, Taphoorn MJ, et al. Radiotherapy plus concomitant and adjuvant temozolomide for glioblastoma. *N Engl J Med*. 2005;352:987–96.
- Louis DN, Ohgaki H, Wiestler OD, Cavenee WK, Burger PC, Jouvet A, et al. The 2007 WHO classification of tumours of the central nervous system. *Acta Neuropathol*. 2007;114:97–109.
- Felsberg J, Rapp M, Loeser S, Fimmers R, Stummer W, Goepfert M, et al. Prognostic significance of molecular markers and extent of resection in primary glioblastoma patients. *Clin Cancer Res*. 2009;15:6683–93.
- Hamacher K, Coenen HH. Efficient routine production of the 18F-labelled amino acid O-2-18F fluoroethyl-L-tyrosine. *Appl Radiat Isot*. 2002;57:853–6.
- Wester HJ, Herz M, Weber W, Heiss P, Senekowitsch-Schmidtke R, Schwaiger M, et al. Synthesis and radiopharmacology of O-(2-[18F]fluoroethyl)-L-tyrosine for tumor imaging. *J Nucl Med*. 1999;40:205–12.
- Langen KJ, Bartenstein P, Boecker H, Brust P, Coenen HH, Drzezga A, et al. German guidelines for brain tumour imaging by PET and SPECT using labelled amino acids. *Nuklearmedizin*. 2011;50:167–73.
- Rapp M, Heinzl A, Galldiks N, Stoffels G, Felsberg J, Ewelt C, et al. Diagnostic performance of 18F-FET PET in newly diagnosed cerebral lesions suggestive of glioma. *J Nucl Med*. 2013;54:229–35.
- Calcagni ML, Galli G, Giordano A, Taralli S, Anile C, Niesen A, et al. Dynamic O-(2-[18F]fluoroethyl)-L-tyrosine (F-18 FET) PET for glioma grading: assessment of individual probability of malignancy. *Clin Nucl Med*. 2011;36:841–7.
- Galldiks N, Stoffels G, Ruge MI, Rapp M, Sabel M, Reifenberger G, et al. Role of O-(2-18F-fluoroethyl)-L-tyrosine PET as a diagnostic tool for detection of malignant progression in patients with low-grade glioma. *J Nucl Med*. 2013;54:2046–54.
- Pauleit D, Floeth F, Hamacher K, Riemenschneider MJ, Reifenberger G, Müller HW, et al. O-(2-[18F]fluoroethyl)-L-tyrosine PET combined with MRI improves the diagnostic assessment of cerebral gliomas. *Brain*. 2005;128:678–87.
- Hutterer M, Nowosielski M, Putzer D, Waitz D, Tinkhauser G, Kostrom H, et al. O-(2-18F-fluoroethyl)-L-tyrosine PET predicts failure of antiangiogenic treatment in patients with recurrent high-grade glioma. *J Nucl Med*. 2011;52:856–64.
- Galldiks N, Rapp M, Stoffels G, Fink GR, Shah NJ, Coenen HH, et al. Response assessment of bevacizumab in patients with recurrent malignant glioma using [18F]fluoroethyl-L-tyrosine PET in comparison to MRI. *Eur J Nucl Med Mol Imaging*. 2013;40:22–33.
- Jansen NL, Suchorska B, Wenter V, Eigenbrod S, Schmid-Tannwald C, Zwergal A, et al. Dynamic 18F-FET PET in newly diagnosed astrocytic low-grade glioma identifies high-risk patients. *J Nucl Med*. 2014;55:198–203.
- Dunet V, Rossier C, Buck A, Stupp R, Prior JO. Performance of 18F-fluoro-ethyl-tyrosine (18F-FET) PET for the differential diagnosis of primary brain tumor: a systematic review and metaanalysis. *J Nucl Med*. 2012;53:207–14.
- Galldiks N, Stoffels G, Filss CP, Piroth MD, Sabel M, Ruge MI, et al. Role of O-(2-18F-fluoroethyl)-L-tyrosine PET for differentiation of local recurrent brain metastasis from radiation necrosis. *J Nucl Med*. 2012;53:1367–74.
- Cha J, Kim ST, Kim HJ, Kim BJ, Kim YK, Lee JY, et al. Differentiation of tumor progression from pseudoprogression in patients with posttreatment glioblastoma using multiparametric histogram analysis. *AJNR Am J Neuroradiol*. 2014;35(7):1309–17.
- Kong DS, Kim ST, Kim EH, Lim DH, Kim WS, Suh YL, et al. Diagnostic dilemma of pseudoprogression in the treatment of newly diagnosed glioblastomas: the role of assessing relative cerebral blood flow volume and oxygen-6-methylguanine-DNA methyltransferase promoter methylation status. *AJNR Am J Neuroradiol*. 2011;32:382–7.
- Mangla R, Singh G, Ziegelitz D, Milano MT, Korones DN, Zhong J, et al. Changes in relative cerebral blood volume 1 month after radiation-temozolomide therapy can help predict overall survival in patients with glioblastoma. *Radiology*. 2010;256:575–84.
- Asao C, Korogi Y, Kitajima M, Hirai T, Baba Y, Makino K, et al. Diffusion-weighted imaging of radiation-induced brain injury for differentiation from tumor recurrence. *AJNR Am J Neuroradiol*. 2005;26:1455–60.
- Hygino da Cruz Jr LC, Rodriguez I, Domingues RC, Gasparetto EL, Sorensen AG. Pseudoprogression and pseudoresponse: imaging challenges in the assessment of posttreatment glioma. *AJNR Am J Neuroradiol*. 2011;32:1978–85.
- Baek HJ, Kim HS, Kim N, Choi YJ, Kim YJ. Percent change of perfusion skewness and kurtosis: a potential imaging biomarker for

- early treatment response in patients with newly diagnosed glioblastomas. *Radiology*. 2012;264:834–43.
36. Kim HS, Kim JH, Kim SH, Cho KG, Kim SY. Posttreatment high-grade glioma: usefulness of peak height position with semiquantitative MR perfusion histogram analysis in an entire contrast-enhanced lesion for predicting volume fraction of recurrence. *Radiology*. 2010;256:906–15.
37. Yoshii Y. Pathological review of late cerebral radionecrosis. *Brain Tumor Pathol*. 2008;25:51–8.